Physics Letters B 756 (2016) 337–344

Contents lists available at ScienceDirect

Physics Letters B

www.elsevier.com/locate/physletb

Renormalizable model for neutrino mass, dark matter, muon $g-2$ and 750 GeV diphoton excess

Hiroshi Okada [a,b,*], Kei Yagyu [c]

[a] School of Physics, KIAS, Seoul 130-722, Republic of Korea
[b] Physics Division, National Center for Theoretical Sciences, Hsinchu, 300, Taiwan
[c] School of Physics and Astronomy, University of Southampton, Southampton, SO17 1BJ, United Kingdom

ARTICLE INFO

Article history:
Received 26 February 2016
Accepted 15 March 2016
Available online 18 March 2016
Editor: J. Hisano

ABSTRACT

We discuss a possibility to explain the 750 GeV diphoton excess observed at the LHC in a three-loop neutrino mass model which has a similar structure to the model by Krauss, Nasri and Trodden. Tiny neutrino masses are naturally generated by the loop effect of new particles with their couplings and masses to be of order 0.1–1 and TeV, respectively. The lightest right-handed neutrino, which runs in the three-loop diagram, can be a dark matter candidate. In addition, the deviation in the measured value of the muon anomalous magnetic moment from its prediction in the standard model can be compensated by one-loop diagrams with exotic multi-charged leptons and scalar bosons. For the diphoton event, an additional isospin singlet real scalar field plays the role to explain the excess by taking its mass of 750 GeV, where it is produced from the gluon fusion production via the mixing with the standard model like Higgs boson. We find that the cross section of the diphoton process can be obtained to be a few fb level by taking the masses of new charged particles to be about 375 GeV and related coupling constants to be order 1.

1. Introduction

In December 2015, the both ATLAS and CMS groups have reported the existence of the excess at around 750 GeV in the diphoton distribution at the Large Hadron Collider (LHC) with the collision energy of 13 TeV. The local significance of this excess is about 3.6σ at ATLAS [1] with the integrated luminosity of 3.2 fb^{-1} and about 2.6σ at CMS [2] with the integrated luminosity of 2.6 fb^{-1}. The detailed properties of the diphoton excess were summarized, e.g., in Ref. [3], where the best fit value of the width of the new resonance is about 45 GeV, and the estimated cross section of the diphoton signature is 10 ± 3 fb at ATLAS and 6 ± 3 fb at CMS. If this excess is confirmed by future data, it suggests the existence of a new particle which gives the direct evidence of a new physics beyond the standard model (SM).

The simplest way to explain this excess is to consider an extension of the SM by adding extra isospin scalar multiplets such as a singlet, a doublet and/or a triplet. However, it is difficult to get a sufficient cross section to explain the excess as mentioned in the above in such a simple extension of the SM. For example, if we consider the CP-conserving two Higgs doublet models (THDMs) [4–7], and take the masses of the additional CP-even H and CP-odd A Higgs bosons to be 750 GeV, then the cross section of $pp \to H/A \to \gamma\gamma$ is typically three order smaller than the required value [4]. Therefore, we need to further introduce additional sources to get an enhancement of the production cross section and/or the branching fraction to the diphoton mode, e.g., by introducing multi-charged scalar particles [4,6] and vector-like fermions [7]. In Refs. [8], the diphoton excess has been discussed in supersymmetric models.

In this paper, we discuss a scenario to *naturally* introduce multi-charged particles to get an enhancement of the branching fraction. Namely, we consider a radiative neutrino mass model in which multi-charged particles play a role not only to increase the branching fraction but also to explain the smallness of neutrino masses and the anomaly of the muon anomalous magnetic moment. A dark matter (DM) candidate can also successfully be involved as a part of the model. There are a few papers discussing the diphoton excess within radiative neutrino mass models [9].

* Corresponding author.
E-mail address: hokada@kias.re.kr (H. Okada).

http://dx.doi.org/10.1016/j.physletb.2016.03.040

Table 1
Particle contents and charge assignments under $SU(2)_L \times U(1)_Y \times Z_2$. The superscripts i and a denote the flavor of the SM fermions and the exotic fermions with $i = 1$–3 and $a = 1$–N_E, respectively.

	Lepton fields					Scalar fields			
	L_L^i	e_R^i	$L_{5/2}^a = (L^{--a}, L^{---a})^T$	E^{--a}	N_R^a	Φ	κ^{++}	S^{++}	Σ
$(SU(2)_L, U(1)_Y)$	$(\mathbf{2}, -1/2)$	$(\mathbf{1}, -1)$	$(\mathbf{2}, -5/2)$	$(\mathbf{1}, -2)$	$(\mathbf{1}, 0)$	$(\mathbf{2}, 1/2)$	$(\mathbf{1}, 2)$	$(\mathbf{1}, 2)$	$(\mathbf{1}, 0)$
Z_2	$+$	$+$	$-$	$-$	$-$	$+$	$+$	$-$	$+$

In particular, we discuss a new three loop neutrino mass model[1] whose structure is similar to the model by Krauss, Nasri and Trodden in 2003 [10], because the three loop suppression factor $1/(16\pi^2)^3$ is a suitable amount to reproduce the measured neutrino masses, i.e., $\mathcal{O}(0.1)$ eV, by order 0.1–1 couplings and TeV scale masses of new particles. In our model, an additional isospin real singlet scalar field can explain the diphoton excess, where it is produced from the gluon fusion process through the mixing with the SM-like Higgs boson.

The plan of the paper is as follows. In Sec. 2, we define our model, and give the Lagrangian for the lepton sector and the scalar potential. In Sec. 3, we discuss the neutrino masses, the phenomenology of DM including the relic abundance and direct search experiments, and new contributions to the muon $g-2$. The diphoton excess is discussed in Sec. 4. Our conclusion is summarized in Sec. 5.

2. The model

Our model is described by the SM gauge symmetry $SU(2)_L \times U(1)_Y$ and an additional discrete symmetry Z_2 which is assumed to be unbroken. This Z_2 symmetry is introduced to avoid tree level contributions to neutrino masses and to enclose the three-loop diagram as shown in Fig. 1. Because of the Z_2 symmetry, the stability of the lightest neutral Z_2 odd particle is guaranteed, and thus it can be a candidate of DM.

The particle contents are shown in Table 1, where L_L^i and e_R^i are the SM left-handed lepton doublets and lepton singlets with the flavor of i ($i = 1$–3). In addition, we add the N_E flavor of the vector like lepton doublets (singlets) $L_{5/2}^a = (L^{--a}, L^{---a})^T$ (E^{--a}) with the hypercharge $Y = -5/2$ (-2) and the right-handed neutrinos N_R^a ($a = 1$–N_E). The scalar sector is composed of one isospin doublet field Φ with $Y = 1/2$ and two complex (one real) isospin singlet scalar fields κ^{++} and S^{++} with $Y = 2$ (Σ with $Y = 0$). The doublet and the real singlet scalar fields are parameterized by

$$\Phi = \begin{pmatrix} G^+ \\ \frac{v+\phi^0+iG^0}{\sqrt{2}} \end{pmatrix}, \quad \Sigma = \sigma^0 + v_\sigma, \tag{1}$$

where v and v_σ are the vacuum expectation values (VEVs) of doublet and singlet scalar fields, respectively, and G^+ (G^0) denotes the Nambu–Goldstone boson which is absorbed into the longitudinal component of the W (Z) boson. The Fermi constant G_F is given by the usual relation, i.e., $G_F = 1/(\sqrt{2}v^2)$ with $v \simeq 246$ GeV. The singlet VEV v_σ does not contribute to the electroweak symmetry breaking. We note that the shift $v_\sigma \to v'_\sigma$ does not change any physical quantities, because its impact can be absorbed by the redefinition of the parameters in the Lagrangian. We thus take $v_\sigma = 0$ in the following discussion to make some expressions to be a simple form.

The most general Lagrangian for the lepton fields is given by

$$\begin{aligned}
-\mathcal{L}_{\rm lep} =& \frac{1}{2} M_N^a \overline{N_R^{ac}} N_R^a + M_L^a \overline{(L_{5/2}^a)_L} (L_{5/2}^a)_R + M_E^a \overline{E_L^{--a}} E_R^{--a} + \text{h.c.} \\
&+ y_{\rm SM}^i \overline{L_L^i} \Phi e_R^i + y_1^{ab} \overline{(L_{5/2}^a)_L} \tilde{\Phi} E_R^{--b} \\
&+ y_2^{ab} \overline{(L_{5/2}^a)_R} \tilde{\Phi} E_L^{--b} + \text{h.c.} \\
&+ g_L^{ab} \overline{(L_{5/2}^a)_L} (L_{5/2}^a)_R \Sigma + g_E^{ab} \overline{(E^{--a})_L} E_R^{--b} \Sigma \\
&+ g_N^{ab} \overline{N_R^{ac}} N_R^b \Sigma + \text{h.c.} \\
&+ h_0^{ij} \overline{e_R^{ic}} e_R^j \kappa^{++} + h_1^{ab} \overline{N_R^a} E_L^{--b} \kappa^{++} + h_2^{ab} \overline{N_R^{ac}} E_R^{--b} \kappa^{++} \\
&+ f^{ia} \overline{L_L^i} (L_{5/2}^a)_R S^{++} + \text{h.c.},
\end{aligned} \tag{2}$$

where $\tilde{\Phi} = i\sigma_2 \Phi^*$. We can take the diagonal form of the invariant masses M_N^a, M_L^a and M_E^a for the vector like leptons $L_{5/2}^a$, E^a and right-handed neutrinos N_R^a, respectively, without loss of generality. The SM leptons L_L and e_R are taken to be the mass eigenstates, so that the Yukawa coupling $y_{\rm SM}^i$ is given by the diagonal form. For simplicity, we assume that all the above parameters are real.

The most general Higgs potential is given by

$$\begin{aligned}
&V(\Phi, \kappa^{++}, S^{++}, \Sigma) \\
&= V_{\rm HSM}(\Phi, \Sigma) + \mu_\kappa^2 (\kappa^{++}\kappa^{--}) + \mu_S^2 (S^{++}S^{--}) \\
&\quad + A_{\Sigma\kappa} \Sigma (\kappa^{++}\kappa^{--}) + A_{\Sigma S} \Sigma (S^{++}S^{--}) \\
&\quad + \lambda_{\Phi\kappa} (\Phi^\dagger\Phi)(\kappa^{++}\kappa^{--}) + \lambda_{\Phi S} (\Phi^\dagger\Phi)(S^{++}S^{--}) \\
&\quad + + \lambda_{\Sigma\kappa} \Sigma^2 (\kappa^{++}\kappa^{--}) \lambda_{\Sigma S} \Sigma^2 (S^{++}S^{--}) \\
&\quad + \lambda_\kappa (\kappa^{++}\kappa^{--})^2 + \lambda_S (S^{++}S^{--})^2 \\
&\quad + + \lambda_{\kappa S} (\kappa^{++}\kappa^{--})(S^{++}S^{--}) \\
&\quad + [\lambda_0 (\kappa^{++}S^{--})(\kappa^{++}S^{--}) + \text{h.c.}],
\end{aligned} \tag{3}$$

where the complex phase of the λ_0 parameter can be absorbed by rephasing the scalar fields. The squared masses of the doubly-charged scalar bosons $S^{\pm\pm}$ and $\kappa^{\pm\pm}$ are given by

$$m_{\kappa^{\pm\pm}}^2 = \mu_\kappa^2 + \frac{v^2}{2}\lambda_{\Phi\kappa}, \quad m_{S^{\pm\pm}}^2 = \mu_S^2 + \frac{v^2}{2}\lambda_{\Phi S}. \tag{4}$$

In Eq. (3), the $V_{\rm HSM}$ part is given in the same form as in the Higgs singlet model (HSM) involving Φ and Σ as

$$\begin{aligned}
V_{\rm HSM}(\Phi, \Sigma) =& \mu_\Phi^2 (\Phi^\dagger\Phi) + \lambda (\Phi^\dagger\Phi)^2 + A_{\Phi\Sigma} (\Phi^\dagger\Phi)\Sigma \\
&+ \lambda_{\Phi\Sigma} (\Phi^\dagger\Phi)\Sigma^2 + t_\Sigma \Sigma + \mu_\Sigma^2 \Sigma^2 \\
&+ A_\Sigma \Sigma^3 + \lambda_\Sigma \Sigma^4.
\end{aligned} \tag{5}$$

Two CP-even scalar states ϕ^0 from the doublet and s^0 from the singlet are mixed with each other via the mixing angle α defined as

$$\begin{pmatrix} \sigma^0 \\ \phi^0 \end{pmatrix} = \begin{pmatrix} \cos\alpha & -\sin\alpha \\ \sin\alpha & \cos\alpha \end{pmatrix} \begin{pmatrix} H \\ h \end{pmatrix}. \tag{6}$$

We define h as the SM-like Higgs boson with the mass of about 125 GeV which is identified as the discovered Higgs boson at the

[1] Other variations of three loop neutrino mass models have also been proposed in Refs. [11–16].

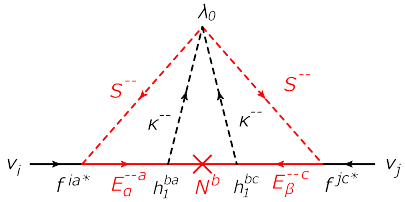

Fig. 1. Three-loop neutrino mass diagram. Particles indicated by the red color are Z_2 odd, where E_α^{--a} and E_β^{--c} denote the mass eigenstates for the doubly-charged exotic leptons. The subscripts α and β (run over 1 and 2) label two mass eigenstates for each flavor. (For interpretation of the references to color in this figure, the reader is referred to the web version of this article.)

LHC. The detailed expressions for the masses of the CP-even Higgs bosons and the mixing angle α in terms of the potential parameters are given, e.g., in Ref. [17].

The masses of the exotic charged leptons are obtained from two sources, i.e., the invariant mass terms M_E and M_L and the Yukawa interaction terms y_1 and y_2. The mass of the triply-charged leptons L^{---a} is simply given by M_L^a. For the doubly-charged leptons, there is a mixing between L^{--a} and E^{--a} through the y_1 and y_2 terms. The mass matrix is given assuming $y_1^{ab} = y_2^{ab} = y_E^a = \mathrm{diag}(y_E^1, \ldots, y_E^{N_E})$ by

$$\begin{aligned}\mathcal{L}_{\rm mass} &= -(\overline{E^{--a}}, \overline{L^{--a}}) \begin{pmatrix} M_E^a & M_D^a \\ M_D^a & M_L^a \end{pmatrix} \begin{pmatrix} E^{--a} \\ L^{--a} \end{pmatrix} \\ &= -(\overline{E_1^{--a}}, \overline{E_2^{--a}}) \begin{pmatrix} M_{E_1}^a & 0 \\ 0 & M_{E_2}^a \end{pmatrix} \begin{pmatrix} E_1^{--a} \\ E_2^{--a} \end{pmatrix}, \end{aligned} \tag{7}$$

where $M_D^a = \frac{v}{\sqrt{2}} y_E^a$. The mass eigenstates E_1^a and E_2^a are defined by the orthogonal transformation:

$$\begin{pmatrix} E^{--a} \\ L^{--a} \end{pmatrix} = \begin{pmatrix} \cos\theta_a & -\sin\theta_a \\ \sin\theta_a & \cos\theta_a \end{pmatrix} \begin{pmatrix} E_1^{--a} \\ E_2^{--a} \end{pmatrix}. \tag{8}$$

The mass eigenvalues ($M_{E_1}^a \le M_{E_2}^a$) and the mixing angles θ_a are given by

$$M_{E_{1,2}}^a = \frac{1}{2}\left(M_E^a + M_L^a \mp \sqrt{(M_E^a - M_L^a)^2 + 4(M_D^a)^2} \right), \tag{9}$$

$$\tan 2\theta_a = \frac{2M_D^a}{M_E^a - M_L^a}. \tag{10}$$

3. Neutrino mass, dark matter, muon $g-2$

3.1. Neutrino mass

The leading contribution to the active neutrino mass matrix m_ν is given at three-loop level as shown in Fig. 1. One- and two-loop diagrams which have been systematically classified in Refs. [18,19] are absent in our setup. The three-loop diagram is computed as follows

$$\begin{aligned}(m_\nu)_{ij} &= \frac{\lambda_0}{(16\pi^2)^3 M_{\rm max}^2} \\ &\times \sum_{a,b,c=1}^{3} \sum_{\alpha,\beta=1}^{2} c_{\alpha\beta} f^{ia*} \sin 2\theta_a M_{E_\alpha}^a h_1^{ba} M_N^b h_1^{bc} \\ &\times \sin 2\theta_c M_{E_\beta}^c f^{jc*} F(r_{E_\alpha^a}, r_{N^b}, r_{E_\beta^c}, r_{S^{\pm\pm}}, r_{\kappa^{\pm\pm}}), \end{aligned} \tag{11}$$

where we define $r_X \equiv (m_X/M_{\rm max})^2$ with $M_{\rm max} = \mathrm{Max}(M_{E_\alpha^a}, M_{E_\beta^c}, M_{N^b}, m_{S^{\pm\pm}}, m_{\kappa^{\pm\pm}})$ and m_X is the mass of a particle X, and $c_{\alpha\beta} = 1\ (-1)$ for $\alpha = \beta$ ($\alpha \neq \beta$). The three loop function F is given by

$$\begin{aligned}&F(r_{E_\alpha^a}, r_{N^b}, r_{E_\beta^c}, r_{S^{\pm\pm}}, r_{\kappa^{\pm\pm}}) \\ &= \int_0^1 dx_1 dy_1 dz_1 \delta(1-x_1-y_1-z_1) \frac{1}{z_1^2 - z_1} \\ &\times \int_0^1 dx_2 dy_2 dz_2 \delta(1-x_2-y_2-z_2) \frac{1}{z_2^2 - z_2} \\ &\times \int_0^1 dx_3 dy_3 dz_3 \delta(1-x_3-y_3-z_3) \frac{1}{\Delta_3}, \end{aligned} \tag{12}$$

where

$$\Delta_3 = x_3 r_{E_\alpha^a} + y_3 r_{S^{\pm\pm}} + z_3 \Delta_2, \tag{13}$$

$$\text{with } \Delta_2 = -\frac{x_2 r_{N^b} + y_2 \Delta_1 + z_2 r_{\kappa^{\pm\pm}}}{z_2^2 - z_2},$$

$$\text{and } \Delta_1 = -\frac{x r_{E_\beta^c} + y r_{S^{\pm\pm}} + z r_{\kappa^{\pm\pm}}}{z_1^2 - z_1}. \tag{14}$$

The interval of the integrals in Eq. (12) for all the variables is from 0 to 1, i.e., $\int_0^1 dxdydz = \int_0^1 dx \int_0^1 dy \int_0^1 dz$. Typical values of F with $r_i = (0.1, 1)$ are $\mathcal{O}(1)$. Let us estimate magnitudes of couplings and masses to reproduce the magnitude of neutrino masses, i.e., the order of 0.1 eV. For simplicity, when we take $M_{\rm max} = M_{E_\alpha^a} \sim M_{E_\beta^c} \sim M_{N^b}$, the neutrino masses are approximately expressed as

$$\begin{aligned}(m_\nu)_{ij} &\sim \frac{M_{\rm max}}{(16\pi^2)^3} \times K_{ij} \\ &\sim (0.1\ \text{eV}) \times 10^6 \times \left(\frac{M_{\rm max}}{v}\right) \times K_{ij}, \end{aligned} \tag{15}$$

$$\text{with } K_{ij} = \sum_{a,b,c=1}^{3} f^{ia*} h_1^{ba} h_1^{bc} f^{jc*}, \tag{16}$$

where we assume $\lambda_0 \times F = \mathcal{O}(1)$. Therefore, in the range of $M_{\rm max} = v$–$10\,v$, the magnitude of the mixing factor K_{ij} is required to be $\mathcal{O}(10^{-7}$–$10^{-6})$.

3.2. Dark matter

Assuming that the right-handed neutrino N_R^1 is the lightest among all the Z_2 odd particles, N_R^1 looses its decay modes into any other lighter particles, and then it becomes stable. We thus can regard N_R^1 as the DM candidate in our model. The annihilation cross section is then calculated as

$$\begin{aligned}\sigma v_{\rm rel} &\approx \int_0^\pi d\theta \sin\theta \\ &\times \int_0^{2\pi} d\phi \frac{1}{128\pi^2 s} |\overline{\mathcal{M}}(N_R^1 N_R^1 \to AB)|^2 \sqrt{1 - \frac{4m_{\rm fin}^2}{s}}, \end{aligned} \tag{17}$$

where $m_{\rm fin}$ is the mass of the final state particle. In the above expression, $|\overline{\mathcal{M}}(N_R^1 N_R^1 \to AB)|^2$ is the squared amplitude for the following two body to two body processes:

$$\begin{aligned}&|\overline{\mathcal{M}}(N_R^1 N_R^1 \to AB)|^2 \\ &= |\overline{\mathcal{M}}(N_R^1 N_R^1 \to \kappa^{++}\kappa^{--})|^2 + |\overline{\mathcal{M}}(N_R^1 N_R^1 \to f\bar{f})|^2 \\ &\quad + |\overline{\mathcal{M}}(N_R^1 N_R^1 \to ZZ)|^2 + |\overline{\mathcal{M}}(N_R^1 N_R^1 \to W^+W^-)|^2 \\ &\quad + |\overline{\mathcal{M}}(N_R^1 N_R^1 \to hh)|^2 + |\overline{\mathcal{M}}(N_R^1 N_R^1 \to HH)|^2. \end{aligned} \tag{18}$$

The first annihilation process $N_R^1 N_R^1 \to \kappa^{++}\kappa^{--}$ happens through the t- and u-channels of the E_α^a mediation, where the doubly-charged scalar boson $\kappa^{\pm\pm}$ decays into the same sign dilepton via the Yukawa coupling h_0. The squared amplitude of the $N_R^1 N_R^1 \to \kappa^{++}\kappa^{--}$ process is given by

$$|\overline{\mathcal{M}}(N_R^1 N_R^1 \to \kappa^{++}\kappa^{--})|^2 = \sum_{a=1}^{N_E} |h^{1a}|^2 \,\mathrm{tr}\left[(\not{p}_2 - M_N^1) X_a (\not{p}_1 + M_N^1) X_a^\dagger\right], \tag{19}$$

$$X_a = \cos^2\theta_a \left[\frac{-\not{p}_1 + \not{k}_1 + M_{E_1}^a}{t - (M_{E_1}^a)^2} + \frac{-\not{p}_1 + \not{k}_2 + M_{E_1}^a}{u - (M_{E_1}^a)^2}\right] + (\cos\theta_a \to \sin\theta_a,\ M_{E_1}^a \to M_{E_2}^a), \tag{20}$$

where s, t and u are the Mandelstam variables, N_c^f is the color factor, and (p_1, p_2) and (k_1, k_2) are the initial and the final state momenta, respectively. In this expression, we take $h^{ab} \equiv h_1^{ab} = h_2^{ab}$ for simplicity. The other cross sections are given through the mixing of α via the s-channel mediation of h and H by

$$|\overline{\mathcal{M}}(N_R^1 N_R^1 \to f\bar{f})|^2 = 16 N_c^f \left(\frac{g_N^{11} m_f s_\alpha c_\alpha}{v}\right)^2 \times \left|\frac{1}{s - m_h^2 + i m_h \Gamma_h} - \frac{1}{s - m_H^2 + i m_H \Gamma_H}\right|^2 \times \left[(p_1\cdot p_2) - (M_N^1)^2\right]\left[(k_1\cdot k_2) - m_f^2\right], \tag{21}$$

$$|\overline{\mathcal{M}}(N_R^1 N_R^1 \to ZZ)|^2 = 8\left(\frac{g_N^{11} m_Z^2 s_\alpha c_\alpha}{v}\right)^2 \left|\frac{1}{s - m_h^2 + i m_h \Gamma_h} - \frac{1}{s - m_H^2 + i m_H \Gamma_H}\right|^2 \times \left[(p_1\cdot p_2) - (M_N^1)^2\right]\left[2 + \frac{(k_1\cdot k_2)^2}{m_Z^4}\right], \tag{22}$$

$$|\overline{\mathcal{M}}(N_R^1 N_R^1 \to W^+W^-)|^2 = 16\left(\frac{g_N^{11} m_W^2 s_\alpha c_\alpha}{v}\right)^2 \times \left|\frac{1}{s - m_h^2 + i m_h \Gamma_h} - \frac{1}{s - m_H^2 + i m_H \Gamma_H}\right|^2 \times \left[(p_1\cdot p_2) - (M_N^1)^2\right]\left[2 + \frac{(k_1\cdot k_2)^2}{m_W^4}\right], \tag{23}$$

$$|\overline{\mathcal{M}}(N_R^1 N_R^1 \to hh)|^2 = 2\left(g_N^{11}\right)^2 \left|\frac{s_\alpha \lambda_{hhh}}{s - m_h^2 + i m_h \Gamma_h} - \frac{c_\alpha \lambda_{Hhh}}{s - m_H^2 + i m_H \Gamma_H}\right|^2 \times \left[(p_1\cdot p_2) - (M_N^1)^2\right], \tag{24}$$

$$|\overline{\mathcal{M}}(N_R^1 N_R^1 \to HH)|^2 = 2\left(g_N^{11}\right)^2 \left|\frac{s_\alpha \lambda_{hHH}}{s - m_h^2 + i m_h \Gamma_h} - \frac{c_\alpha \lambda_{HHH}}{s - m_H^2 + i m_H \Gamma_H}\right|^2 \times \left[(p_1\cdot p_2) - (M_N^1)^2\right], \tag{25}$$

where we use the short-hand notations of $c_\alpha \equiv \cos\alpha$ and $s_\alpha \equiv \sin\alpha$. The dimensionful $\lambda_{\varphi_i\varphi_j\varphi_k}$ couplings ($\varphi_{i,j,k} = h$ or H) are defined by the coefficient of the scalar trilinear vertex in the potential. We note that the s-wave contribution to $\sigma v_{\rm rel}$ vanishes due to the Majorana property of the DM. To reproduce the observed relic density, the cross section given in Eq. (17) should be inside the following region

$$\sigma v_{\rm rel} = (1.78\text{–}1.97) \times 10^{-9}\ \mathrm{GeV}^{-2}, \tag{26}$$

at the 2σ level [20].

We also consider the spin independent scattering cross section with a neutron that is induced via the tree level diagram with the Higgs boson h and H exchange. The formula is given by

$$\sigma_{\rm SI}^n = \frac{C^2}{\pi}\left(\frac{m_n^2 M_N^1}{m_n + M_N^1}\right)^2 \left(\frac{g_N^{11} c_\alpha s_\alpha}{v}\right)^2 \left(-\frac{1}{m_h^2} + \frac{1}{m_H^2}\right)^2, \tag{27}$$

where the neutron mass is $m_n \simeq 0.939$ GeV and the factor $C \simeq 0.287^2$ is determined by the lattice simulation. The latest upper bound is reported by the LUX experiment that suggests $\sigma_{\rm SI}^n \lesssim 10^{-45}$ cm for the DM mass of about 100 GeV with the 90% C.L. [21].

3.3. Muon $g-2$

The muon anomalous magnetic moment (muon $g-2$) is one of the most promising low energy observables which suggest the existence of new physics beyond the SM. This is because there is the more than 3σ deviation in the SM prediction from the experimental value measured at Brookhaven National Laboratory. The difference $\Delta a_\mu \equiv a_\mu^{\rm exp} - a_\mu^{\rm SM}$ has been calculated in Ref. [22] as

$$\Delta a_\mu = (29.0 \pm 9.0) \times 10^{-10}. \tag{28}$$

This shows the 3.2σ deviation in the SM prediction.

In our model, two diagrams contribute to Δa_μ, where L^{---a}–S^{--a} and ℓ^-–κ^{--a} with ℓ^- being the SM lepton are running in the loop. These contributions are calculated by

$$\Delta a_\mu \simeq \frac{m_\mu^2}{16\pi^2}\left\{\sum_{a=1}^{N_E} |f^{\mu a}|^2 \left[\frac{3}{M_L^{a2}} G\left(\frac{m_{S^{\pm\pm}}^2}{M_L^{a2}}\right) + \frac{2}{m_{S^{\pm\pm}}^2} G\left(\frac{M_L^{a2}}{m_{S^{\pm\pm}}^2}\right)\right] - \sum_{i=1}^{3} |\bar{h}_0^{\mu i}|^2 \frac{2}{3 m_{\kappa^{\pm\pm}}^2}\right\} \tag{29}$$

where $\bar{h}_0^{ij} = h_0^{ij}\,(2h_0^{ij})$ for $i = j$ $(i \neq j)$, and

$$G(x) = \frac{1 - 6x + 3x^2 + 2x^3 - 6x^2 \ln x}{(1-x)^4}. \tag{30}$$

We can see that the contribution from the $\kappa^{\pm\pm}$ loop gives the negative value which is undesired to explain the muon $g-2$ anomaly. We thus neglect the $\kappa^{\pm\pm}$ loop contribution that can be realized by taking $\bar{h}_0^{\mu i} \ll f^{\mu a}$.

3.4. A set of solution

Here, we show a set of the solution to give the sizable amount of Δa_μ, i.e., $2.0 \times 10^{-9} \lesssim \Delta a_\mu \lesssim 3.8 \times 10^{-9}$, the non-relativistic cross section to satisfy the observed relic density $\sigma v_{\rm rel} = (1.78\text{–}1.97) \times 10^{-9}$ GeV^{-2}, and to satisfy the constraint of the direct detection $\sigma_{\rm SI}^n \lesssim 10^{-45}$, where we conservatively take the constraint of the direct detection for all the mass region of DM. By taking the number of the flavor $N_E = 3$, we find the following benchmark parameter sets:

$$m_{\kappa^{\pm\pm}} = 375\ \text{GeV}, \quad m_{S^{\pm\pm}} = 377\ \text{GeV},$$
$$M_{E_1} = 375\ \text{GeV}, \quad M_{E_2} = 380\ \text{GeV},$$
$$M_N^1 = 478\ \text{GeV}, \quad M_N^{2,3} = 556\ \text{GeV},$$
$$m_H = 750\ \text{GeV}, \quad \Gamma_H = 2.40\ \text{GeV},$$
$$\sum_{a=1}^{3} |f^{\mu a}|^2 = 3.04^2, \quad \sum_{a=1}^{3} |h^{1a}|^2 = 0.721^2,$$
$$g_N^{11} = 1.06 \times 10^{-3}, \quad \sin\theta_E = 0.141, \quad \sin\alpha = -0.1, \tag{31}$$

where $M_{E_{1,2}} = M^a_{E_{1,2}}$, $\theta_E = \theta_a$ for a = 1-3, and we take $\lambda_{hhh} = \lambda_{Hhh} = 0$. The triply-charged lepton mass M_L is given about 375 GeV from the above inputs. The values for three parameters m_H, $\sin\alpha$ and Γ_H are favored for the discussion of the 750 GeV diphoton signature which will be discussed in the next section. The other SM parameters are fixed as follows

$$\Gamma_h = 4.1\ \text{MeV}, \quad m_h = 125.5\ \text{GeV}, \quad v = 246\ \text{GeV},$$
$$m_W = 80.4\ \text{GeV}, \quad m_Z = 91.2\ \text{GeV},$$
$$m_t = 173\ \text{GeV}, \quad m_b = 4.18\ \text{GeV}. \tag{32}$$

From the benchmark set, we obtain the following results

$$\Delta a_\mu = 3.54 \times 10^{-9}, \quad \sigma v_{\rm rel} = 1.87 \times 10^{-9}\ \text{GeV}^{-2}. \tag{33}$$

4. Diphoton excess

We discuss how we can reproduce the diphoton excess at around 750 GeV at the LHC. In our model, the additional CP-even Higgs boson H plays the role to explain this excess via the gluon fusion production process by taking its mass of 750 GeV. The cross section $\sigma_{\gamma\gamma}$ of the diphoton channel is expressed by using the narrow width approximation as follows

$$\sigma_{\gamma\gamma} \equiv \sigma(gg \to H \to \gamma\gamma) \simeq \sigma(gg \to H) \times \mathcal{B}(H \to \gamma\gamma). \tag{34}$$

Non-zero production cross section $\sigma(gg \to H)$ of the gluon fusion process is given through the mixing α with the SM-like Higgs boson h defined in Eq. (6) as

$$\sigma(gg \to H) = \sin^2\alpha \times \sigma(gg \to h_{\rm SM}), \tag{35}$$

where $h_{\rm SM}$ denotes the SM Higgs boson, and $\sigma(gg \to h_{\rm SM})$ does its gluon fusion cross section in which the mass of $h_{\rm SM}$ here is fixed to be 750 GeV in order to derive the cross section for H. From [23], we obtain $\sigma(gg \to h_{\rm SM}) \simeq 736$ fb at the collision energy of 13 TeV.

Next, we discuss the decays of H and h to figure out the branching fraction of $\mathcal{B}(H \to \gamma\gamma)$ and the signal strength μ_{XY} of $pp \to h \to XY$ modes for h. The latter quantity becomes important to set a constraint on the parameter space. In particular, when we consider the enhancement of $\mathcal{B}(H \to \gamma\gamma)$, this could also significantly modify the event rates of h for various channels. The definition of μ_{XY} is given by

$$\mu_{XY} = \sigma(gg \to h) \times \mathcal{B}(h \to XY). \tag{36}$$

The decay rates of $\mathcal{H} \to \mathcal{P}\mathcal{P}'$ with $\mathcal{H} = h$ or H and $\mathcal{P}\mathcal{P}' = f\bar{f}$, W^+W^-, ZZ or gg are given by

$$\Gamma(\mathcal{H} \to \mathcal{P}\mathcal{P}') = \xi^2_{\mathcal{H}} \Gamma(h_{\rm SM} \to \mathcal{P}\mathcal{P}'), \tag{37}$$

where $\xi_{\mathcal{H}} = \sin\alpha$ $(\cos\alpha)$ for $\mathcal{H} = H$ (h). For the $\gamma\gamma$ and $Z\gamma$ modes, the decay rate is not simply given by the above way due to the additional loop contributions of the new charged particles. In order to simplify the discussion, we take flavor universal valuables for the masses of the exotic charged leptons and the mixing angles, i.e., $M^a_{E_\alpha} = M_{E_\alpha}$ and $\theta_a = \theta_E$ as we have done it in the previous section. In this case, the decay rates for $\mathcal{H} \to \gamma\gamma$ and $\mathcal{H} \to Z\gamma$ are given by

$$\begin{aligned}
&\Gamma(\mathcal{H} \to \gamma\gamma) \\
&= \frac{\sqrt{2} G_F \alpha_{\rm em}^2 m_{\mathcal{H}}^3}{256\pi^3} \\
&\quad \times \Bigg| \xi_{\mathcal{H}} F_{\rm SM} - Q_{2+}^2 \sum_{\phi=S,\kappa} \frac{\lambda_{\mathcal{H}\phi^{++}\phi^{--}}}{v} F_0^{\mathcal{H}}(m_{\phi^{\pm\pm}}) \\
&\quad + \bar{\xi}_{\mathcal{H}} Q_{3-}^2 N_E g_S \left(\frac{v}{M_L}\right) F_{1/2}^{\mathcal{H}}(M_L) \\
&\quad + Q_{2-}^2 N_E \sum_{\alpha=1,2} y_{\mathcal{H}E_\alpha E_\alpha} \left(\frac{v}{M_{E_\alpha}}\right) F_{1/2}^{\mathcal{H}}(M_{E_\alpha}) \Bigg|^2,
\end{aligned} \tag{38}$$

$$\begin{aligned}
&\Gamma(\mathcal{H} \to Z\gamma) \\
&= \frac{\sqrt{2} G_F \alpha_{\rm em}^2 m_h^3}{128\pi^3} \left(1 - \frac{m_Z^2}{m_h^2}\right)^3 \\
&\quad \times \Bigg| \xi_{\mathcal{H}} G_{\rm SM} - (-s_W^2 Q_{2+}^2) \sum_{\phi=S,\kappa} \frac{\lambda_{\mathcal{H}\phi^{++}\phi^{--}}}{v} G_0^{\mathcal{H}}(m_{\phi^{\pm\pm}}) \\
&\quad + \bar{\xi}_{\mathcal{H}} Q_{3-}(-1/2 - s_W^2 Q_{3-}) N_E g_S \left(\frac{v}{M_L}\right) G_{1/2}^{\mathcal{H}}(M_L) \\
&\quad + Q_{2-} \left(\frac{\sin^2\theta_E}{2} - s_W^2 Q_{2-}\right) N_E\, y_{\mathcal{H}E_1E_1} \left(\frac{v}{M_{E_1}}\right) G_{1/2}^{\mathcal{H}}(M_{E_1}) \\
&\quad + Q_{2-} \left(\frac{\cos^2\theta_E}{2} - s_W^2 Q_{2-}\right) N_E\, y_{\mathcal{H}E_2E_2} \left(\frac{v}{M_{E_2}}\right) G_{1/2}^{\mathcal{H}}(M_{E_2}) \\
&\quad + Q_{2-} \frac{\sin 2\theta_E}{4} N_E\, y_{\mathcal{H}E_1E_2} G_{1/2}^{\mathcal{H}}(M_{E_1}, M_{E_2}) \Bigg|^2,
\end{aligned} \tag{39}$$

where $\bar{\xi}_{\mathcal{H}} = \cos\alpha$ $(-\sin\alpha)$ for $\mathcal{H} = H$ (h) and Q_X denotes the electric charge, i.e., $Q_t = 2/3$, $Q_b = -1/3$, $Q_{3-} = -3$ and $Q_{2\pm} = \pm 2$. In the above formulae, the Yukawa couplings $y_{\mathcal{H}E_\alpha E_\beta}$ and the scalar trilinear couplings $\lambda_{\mathcal{H}\phi^{++}\phi^{--}}$ are given by

$$y_{\mathcal{H}E_1E_1} = \frac{y_E}{\sqrt{2}} \xi_{\mathcal{H}} \sin 2\theta_E + g_S \bar{\xi}_{\mathcal{H}}, \tag{40}$$
$$y_{\mathcal{H}E_2E_2} = -\frac{y_E}{\sqrt{2}} \xi_{\mathcal{H}} \sin 2\theta_E + g_S \bar{\xi}_{\mathcal{H}}, \tag{41}$$
$$y_{\mathcal{H}E_1E_2} = \frac{y_E}{\sqrt{2}} \xi_{\mathcal{H}} \cos 2\theta_E, \tag{42}$$
$$\lambda_{\mathcal{H}\kappa^{++}\kappa^{--}} = -(v\lambda_{\Phi\kappa}\xi_{\mathcal{H}} + A_{\Sigma\kappa}\bar{\xi}_{\mathcal{H}}), \tag{43}$$
$$\lambda_{\mathcal{H}S^{++}S^{--}} = -(v\lambda_{\Phi S}\xi_{\mathcal{H}} + A_{\Sigma S}\bar{\xi}_{\mathcal{H}}). \tag{44}$$

The contribution of the SM particles to $\mathcal{H} \to \gamma\gamma$ ($F_{\rm SM}$) and $\mathcal{H} \to Z\gamma$ ($G_{\rm SM}$) are expressed as

$$F_{\rm SM} = F_1^{\mathcal{H}}(m_W) + 3 \sum_{f=t,b} Q_f^2 F_{1/2}^{\mathcal{H}}(m_f), \tag{45}$$
$$G_{\rm SM} = G_1^{\mathcal{H}}(m_W) + 3 \sum_{f=t,b} Q_f \left(\frac{I_f}{2} - s_W^2 Q_f\right) G_{1/2}^{\mathcal{H}}(m_f), \tag{46}$$

with $I_f = 1/2$ $(-1/2)$ for $f = t$ (b). The loop functions for the $\gamma\gamma$ mode are expressed by

$$F_0^{\mathcal{H}}(m_\varphi) = \frac{2v^2}{m_{\mathcal{H}}^2}[1 + 2m_{\phi^\pm}^2 C_0(0, 0, m_{\mathcal{H}}^2, m_\varphi, m_\varphi, m_\varphi)], \tag{47}$$

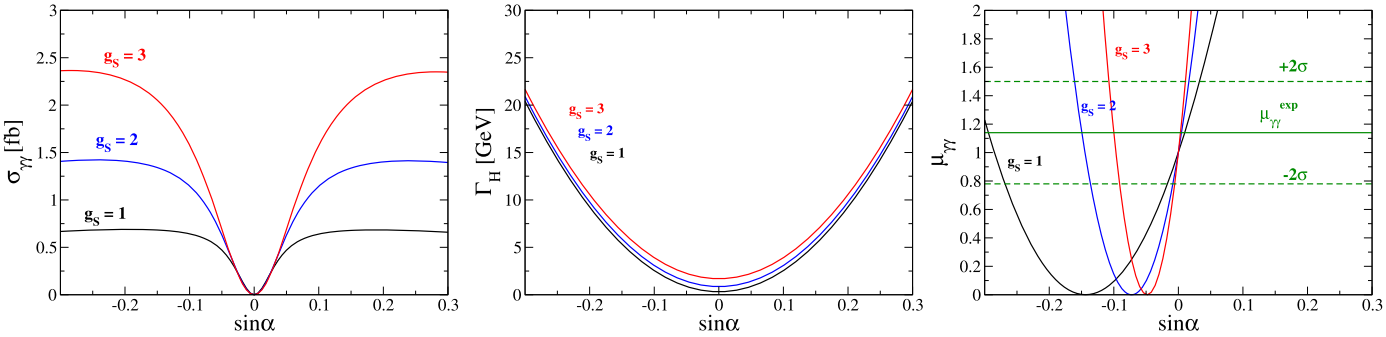

Fig. 2. The $\sin\alpha$ dependence of the cross section $\sigma_{\gamma\gamma}$ for the diphoton process (left), the total width Γ_H of H and the signal strength $\mu_{\gamma\gamma}$ (right). We take $N_E = 3$ and $\lambda_{\mathcal{H}S^{++}S^{--}} = \lambda_{\mathcal{H}\kappa^{++}\kappa^{--}} = 0$. The black, blue and red curves show the case of $g_S = 1, 2$ and 3, respectively. For the right panel, the central value of and the 2σ limit on $\mu_{\gamma\gamma}$ from the LHC Run-I experiment are also shown as the green horizontal lines. (For interpretation of the references to color in this figure, the reader is referred to the web version of this article.)

$$F_{1/2}^{\mathcal{H}}(m_F) = -\frac{4m_F^2}{m_{\mathcal{H}}^2}\left[2 - m_{\mathcal{H}}^2\left(1 - \frac{4m_F^2}{m_{\mathcal{H}}^2}\right)C_0(0,0,m_{\mathcal{H}}^2,m_F,m_F,m_F)\right], \tag{48}$$

$$F_1^{\mathcal{H}}(m_W) = \frac{2m_W^2}{m_{\mathcal{H}}^2}\left[6 + \frac{m_{\mathcal{H}}^2}{m_W^2} + (12m_V^2 - 6m_{\mathcal{H}}^2)C_0(0,0,m_{\mathcal{H}}^2,m_W,m_W,m_W)\right], \tag{49}$$

and those for the $Z\gamma$ mode are given by

$$G_0^{\mathcal{H}}(m_\varphi) = \frac{2v^2}{e(m_{\mathcal{H}}^2 - m_Z^2)}\left\{1 + 2m_\varphi^2 C_0(0,m_Z^2,m_{\mathcal{H}}^2,m_\varphi,m_\varphi,m_\varphi) + \frac{m_Z^2}{m_{\mathcal{H}}^2 - m_Z^2}\left[B_0(m_{\mathcal{H}}^2,m_\varphi,m_\varphi) - B_0(m_Z^2,m_\varphi,m_\varphi)\right]\right\}, \tag{50}$$

$$G_{1/2}^{\mathcal{H}}(m_F) = \frac{4m_F^2}{s_W c_W}(4C_{23} + 4C_{12} + C_0)(0,m_Z^2,m_{\mathcal{H}}^2,m_F,m_F,m_F), \tag{51}$$

$$G_{1/2}^{\mathcal{H}}(m_{F_1},m_{F_2}) = \frac{4v}{s_W c_W}\left[2(m_{F_1}+m_{F_2})C_{23} + 2(m_{F_1}+m_{F_2})C_{12} + m_{F_1}C_0\right](0,m_Z^2,m_{\mathcal{H}}^2,m_{F_1},m_{F_2},m_{F_2}) + (F_1 \leftrightarrow F_2), \tag{52}$$

$$G_1^{\mathcal{H}}(m_W) = \frac{2m_W^2}{s_W c_W (m_h^2 - m_Z^2)}\left\{\left[c_W^2\left(5 + \frac{m_{\mathcal{H}}^2}{2m_W^2}\right) - s_W^2\left(1 + \frac{m_{\mathcal{H}}^2}{2m_W^2}\right)\right]\left[1 + \frac{m_Z^2}{m_{\mathcal{H}}^2 - m_W^2}(B_0(m_{\mathcal{H}}^2,m_W,m_W) - B_0(m_Z^2,m_W,m_W))\right] + [2m_W^2 - 6c_W^2(m_{\mathcal{H}}^2 - m_Z^2) + 2s_W^2(m_{\mathcal{H}}^2 - m_Z^2)]C_0(0,m_Z^2,m_{\mathcal{H}}^2,m_W,m_W,m_W)\right\}, \tag{53}$$

where B_i and C_{ij} are the two- and three-point Passarino–Veltman functions [24], respectively. The notation for these functions is the same as that in Ref. [25]. In addition to the above mentioned decay modes, the $H \to hh$ mode is generally allowed. However, this mode typically reduces the branching fraction of the $H \to \gamma\gamma$ channel to one order, and it makes difficult to explain the observed cross section of the diphoton signature. We thus assume that the decay rate of this process is zero by taking the dimensionful Hhh coupling to be zero.

Let us perform the numerical analysis to show our predictions of the cross section $\sigma_{\gamma\gamma}$ for the diphoton process $gg \to H \to \gamma\gamma$, the total width Γ_H of H and the signal strength μ_{XY}. In the following analysis, we take the mixing angle θ_E to be zero (equivalently taking $y_E = 0$), where a non-zero value of θ_E does not give an important change of the value of $\Gamma(\mathcal{H} \to \gamma\gamma)$ and $\Gamma(\mathcal{H} \to Z\gamma)$. We also take all the masses of the exotic leptons and the doubly-charged scalar bosons to be 375 GeV which maximizes the value of $\Gamma(H \to \gamma\gamma)$ for a given set of other fixed parameters.

In Fig. 2, we show the $\sin\alpha$ dependence for the diphoton cross section $\sigma_{\gamma\gamma}$ (left panel), the total width Γ_H (center panel) and the signal strength $\mu_{\gamma\gamma}$ (right panel) in the case of the number of flavor of the exotic leptons N_E to be 3. In these plots, we take $\lambda_{\mathcal{H}S^{++}S^{--}} = \lambda_{\mathcal{H}\kappa^{++}\kappa^{--}} = 0$, in which only the exotic leptons give the additional contributions to the $\mathcal{H} \to \gamma\gamma$ and $\mathcal{H} \to Z\gamma$ decays. The value of the Yukawa coupling g_S is taken to be 1, 2 and 3 in all the panels. For the right panel, the measured value of $\mu_{\gamma\gamma}$, i.e., $\mu_{\gamma\gamma}^{\rm exp} = 1.14 \pm 0.76$ [26] at the LHC Run-I experiment is also shown, where the solid and dashed curves denote the central value and the 2σ limit, respectively. We obtain the cross section to be about 0.6, 1.4 and 2.4 fb when $|\sin\alpha| \gtrsim 0.1, 0.15$ and 0.2 in the case of $g_S = 1, 2$ and 3, respectively. Regarding to the width Γ_H, its value strongly depends on $\sin\alpha$, while the dependence on g_S is quite weak. We find that $\Gamma_H \simeq 2.4$ (8.5) GeV at $|\sin\alpha| = 0.1$ (0.2) with $g_S = 1$. For $\sigma_{\gamma\gamma}$ and Γ_H, the sign of $\sin\alpha$ does not become important so much, while that for $\mu_{\gamma\gamma}$ does quite important. This can be understood in such a way that the interference effect in the $h \to \gamma\gamma$ process between the W boson loop and the exotic lepton loops becomes constructive (destructive) when $\sin\alpha$ is positive (negative). Because of this destructive effect, the value of $\mu_{\gamma\gamma}$ becomes zero at $\sin\alpha \lesssim 0$, and it rapidly grows when $\sin\alpha$ is taken to be a different value from that giving $\mu_{\gamma\gamma} = 0$. Therefore, the case with $\sin\alpha$ taken to be a bit different value from that giving $\mu_{\gamma\gamma} = 0$ is allowed by the current experimental data $\mu_{\gamma\gamma}^{\rm exp}$. For the other signal strengths which have been measured at LHC, i.e., μ_{ZZ}, μ_{WW} and $\mu_{\tau\tau}$, they are calculated by $\cos^2\alpha$ at the tree level. In the range of $\sin\alpha$ that we take in Fig. 2, we obtain $\cos^2\alpha > 0.91$, so that these signal strengths are allowed at the 2σ level from the LHC Run-I data [27,28].

In Fig. 3, we show the contour plots of $\sigma_{\gamma\gamma}$ on the $\sin\alpha$–g_S plane in the case of $\lambda_{\mathcal{H}S^{++}S^{--}} = \lambda_{\mathcal{H}\kappa^{++}\kappa^{--}} = 0$. The left, center and right panels respectively show the case of $N_E = 3, 6$ and 9. We restrict the range of $\sin\alpha$ to be 0 to -0.3, because the positive

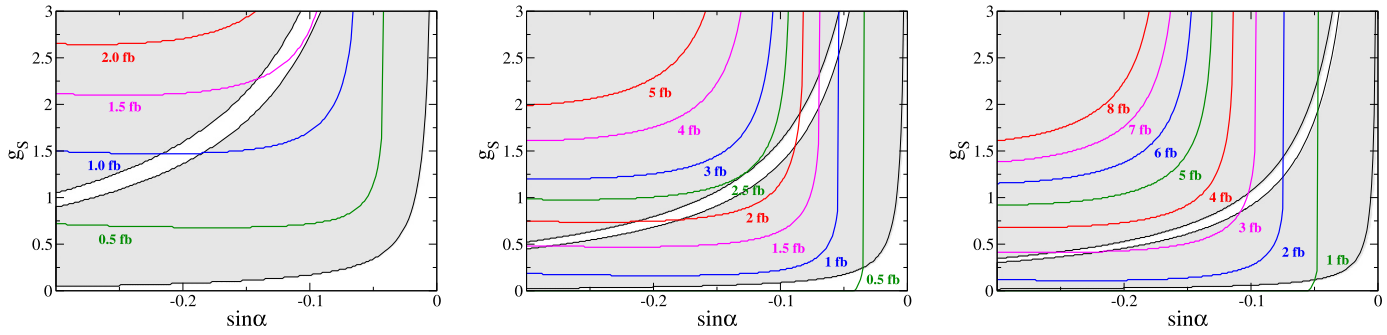

Fig. 3. Contour plots for the cross section $\sigma_{\gamma\gamma}$ on the $\sin\alpha$–g_S plane. We take $\lambda_{\mathcal{H}S^{++}S^{--}} = \lambda_{\mathcal{H}\kappa^{++}\kappa^{--}} = 0$. The left, center and right panels respectively show the case of $N_E = 3, 6$ and 9. (For interpretation of the references to color in this figure, the reader is referred to the web version of this article.)

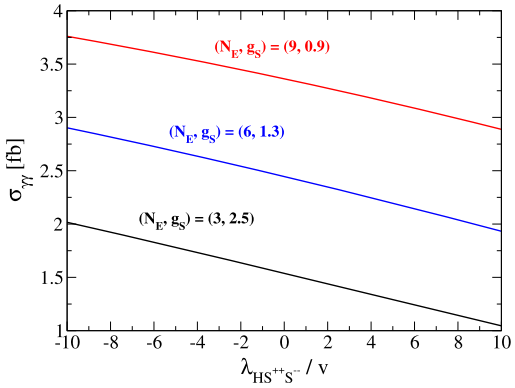

Fig. 4. Cross section $\sigma_{\gamma\gamma}$ as a function of $\lambda_{HS^{++}S^{--}}/v$. We take $\lambda_{H\kappa^{++}\kappa^{--}} = \lambda_{HS^{++}S^{--}}$ and $\lambda_{h\kappa^{++}\kappa^{--}} = \lambda_{hS^{++}S^{--}} = 0$. The black, blue and red curves respectively show the case of $(N_E, g_S) = (3, 2.5)$, $(6, 1.3)$ and $(9, 0.9)$. For all the plots, we take $\sin\alpha = -0.12$. (For interpretation of the references to color in this figure, the reader is referred to the web version of this article.)

value of $\sin\alpha$ is highly disfavored by $\mu^{\rm exp}_{\gamma\gamma}$ as we see in Fig. 2. The shaded region is excluded by $\mu^{\rm exp}_{\gamma\gamma}$ at the 2σ level. We find that the maximally allowed value of the cross section $\sigma_{\gamma\gamma}$ is about 1.5 fb, 2.5 fb and 3 fb when N_E is taken to be 3, 6 and 9, respectively.

Finally, we add the non-zero contributions to $\mathcal{H} \to \gamma\gamma$ from the doubly-charged scalar bosons $S^{\pm\pm}$ and $\kappa^{\pm\pm}$. In Fig. 4, we show the diphoton cross section $\sigma_{\gamma\gamma}$ as a function of $\lambda_{HS^{++}S^{--}}$ $(= \lambda_{H\kappa^{++}\kappa^{--}})$ normalized by v in the case of $\lambda_{hS^{++}S^{--}} = \lambda_{h\kappa^{++}\kappa^{--}}$. In this case, only the $H \to \gamma\gamma/Z\gamma$ mode is modified as compared to the previous cases shown in Figs. 2 and 3 for the same parameter choice of N_E and g_S. In this figure, we take $(N_E, g_S) = (3, 2.5)$, (6,1.3) and (9,0.9), and $\sin\alpha = -0.12$ for these three cases, where these points give the maximal allowed value of $\sigma_{\gamma\gamma}$ that is found in Fig. 3. We can see that the constructive effect between the exotic lepton loops and the doubly-charged scalar boson loops is obtained when $\lambda_{hS^{++}S^{--}} < 0$. At $\lambda_{hS^{++}S^{--}}/v = -10$, we obtain $\sigma_{\gamma\gamma} \simeq 2.0, 2.8$ and 3.8 fb at $(N_E, g_S) = (3, 2.5), (6, 1.3)$ and $(9, 0.9)$, respectively.

5. Conclusions

We have constructed the three-loop neutrino mass model whose structure is similar to the model by Krauss, Nasri and Trodden. The neutrino masses of $\mathcal{O}(0.1)$ eV are naturally generated by the loop effect of new particles with their couplings and masses to be of order 0.1–1 and TeV, respectively. We have analyzed the Majorana DM candidate, assuming the lightest of N_R. The non-relativistic cross section to explain the observed relic density is p-wave dominant, and there are several processes; $N^1_R N^1_R \to \kappa^{++}\kappa^{--}$ with the t- and u-channels, and $N^1_R N^1_R \to f\bar{f}$, $N^1_R N^1_R \to ZZ$, $N^1_R N^1_R \to W^+W^-$, $N^1_R N^1_R \to hh$, $N^1_R N^1_R \to HH$ with the s-channel. The dominant DM scattering with a nucleus comes from the Higgs boson mediation h and H at the tree level, and we have calculated the spin independent cross section of the process. Furthermore, the anomaly of the muon $g-2$ can be solved by the one-loop contribution of the triply-charged exotic leptons and doubly-charged scalar boson. We have found the benchmark parameter set to satisfy the relic abundance of the DM, the constraint from the direct search experiment and to compensate the deviation in the measured value of the muon $g-2$ from the SM prediction.

We then have numerically shown the cross section of the diphoton process via the gluon fusion production $gg \to H \to \gamma\gamma$ and the width of H under the constraint from the signal strength $\mu_{\gamma\gamma}$ for the SM-like Higgs boson measured at the LHC Run-I experiment. We have obtained the width to be about 3–5 GeV in the typical parameter region, which gives a tension to the measured value, i.e., about 45 GeV. We have found that the cross section of the diphoton process is given to be a few fb level by taking the masses of new charged fermions and scalar bosons to be 375 GeV with an order 1 coupling constant. A bit larger cross section such as about 4 fb is obtained by taking the larger number of flavor N_E of the exotic leptons and take a non-zero negative value of the trilinear scalar boson couplings $\lambda_{HS^{++}S^{--}}$ and $\lambda_{H\kappa^{++}\kappa^{--}}$.

Acknowledgements

H.O. expresses his sincere gratitude toward all the KIAS members, Korean cordial persons, foods, culture, weather, and all the other things. K.Y. is supported by JSPS postdoctoral fellowships for research abroad.

References

[1] ATLAS Collaboration, ATLAS-CONF-2015-081.
[2] CMS Collaboration, EXO-PAS-15-004.
[3] R. Franceschini, et al., arXiv:1512.04933 [hep-ph].
[4] S. Moretti, K. Yagyu, arXiv:1512.07462 [hep-ph].
[5] S. Di Chiara, L. Marzola, M. Raidal, arXiv:1512.04939 [hep-ph].
[6] X.F. Han, L. Wang, arXiv:1512.06587 [hep-ph].
[7] A. Angelescu, A. Djouadi, G. Moreau, arXiv:1512.04921 [hep-ph];
R.S. Gupta, S. Jager, Y. Kats, G. Perez, E. Stamou, arXiv:1512.05332 [hep-ph];
D. Becirevic, E. Bertuzzo, O. Sumensari, R.Z. Funchal, arXiv:1512.05623 [hep-ph];
M. Badziak, arXiv:1512.07497 [hep-ph];
N. Bizot, S. Davidson, M. Frigerio, J.-L. Kneur, arXiv:1512.08508 [hep-ph];
A.E.C. Hernández, I.d.M. Varzielas, E. Schumacher, arXiv:1601.00661 [hep-ph];
A. Djouadi, J. Ellis, R. Godbole, J. Quevillon, arXiv:1601.03696 [hep-ph].
[8] E. Gabrielli, K. Kannike, B. Mele, M. Raidal, C. Spethmann, H. Veermae, arXiv:1512.05961 [hep-ph];
L.M. Carpenter, R. Colburn, J. Goodman, arXiv:1512.06107 [hep-ph];
R. Ding, L. Huang, T. Li, B. Zhu, arXiv:1512.06560 [hep-ph];
M.x. Luo, K. Wang, T. Xu, L. Zhang, G. Zhu, arXiv:1512.06670 [hep-ph];

T.F. Feng, X.Q. Li, H.B. Zhang, S.M. Zhao, arXiv:1512.06696 [hep-ph];
F. Wang, L. Wu, J.M. Yang, M. Zhang, arXiv:1512.06715 [hep-ph];
B.C. Allanach, P.S.B. Dev, S.A. Renner, K. Sakurai, arXiv:1512.07645 [hep-ph].
[9] S. Kanemura, K. Nishiwaki, H. Okada, Y. Orikasa, S.C. Park, R. Watanabe, arXiv:1512.09048 [hep-ph];
T. Nomura, H. Okada, arXiv:1601.00386 [hep-ph];
J.H. Yu, arXiv:1601.02609 [hep-ph];
R. Ding, Z.L. Han, Y. Liao, X.D. Ma, arXiv:1601.02714 [hep-ph];
T. Nomura, H. Okada, arXiv:1601.04516 [hep-ph].
[10] L.M. Krauss, S. Nasri, M. Trodden, Phys. Rev. D 67 (2003) 085002.
[11] M. Aoki, S. Kanemura, O. Seto, Phys. Rev. Lett. 102 (2009) 051805;
M. Aoki, S. Kanemura, K. Yagyu, Phys. Rev. D 83 (2011) 075016, arXiv:1102.3412 [hep-ph].
[12] M. Gustafsson, J.M. No, M.A. Rivera, Phys. Rev. Lett. 110 (21) (2013) 211802;
M. Gustafsson, J.M. No, M.A. Rivera, Phys. Rev. Lett. 112 (25) (2014) 259902.
[13] Y. Kajiyama, H. Okada, K. Yagyu, J. High Energy Phys. 1310 (2013) 196.
[14] P. Culjak, K. Kumericki, I. Picek, Phys. Lett. B 744 (2015) 237.
[15] H. Okada, K. Yagyu, Phys. Rev. D 93 (1) (2016) 013004, arXiv:1508.01046 [hep-ph].
[16] K. Nishiwaki, H. Okada, Y. Orikasa, Phys. Rev. D 92 (9) (2015) 093013, arXiv:1507.02412 [hep-ph].
[17] S. Kanemura, M. Kikuchi, K. Yagyu, arXiv:1511.06211 [hep-ph].
[18] D. Aristizabal Sierra, A. Degee, L. Dorame, M. Hirsch, J. High Energy Phys. 1503 (2015) 040.
[19] Y. Farzan, S. Pascoli, M.A. Schmidt, J. High Energy Phys. 1303 (2013) 107.
[20] P.A.R. Ade, et al., Planck Collaboration, Astron. Astrophys. 571 (2014) A16.
[21] D.S. Akerib, et al., LUX Collaboration, Phys. Rev. Lett. 112 (2014) 091303.
[22] F. Jegerlehner, A. Nyffeler, Phys. Rep. 477 (2009) 1.
[23] https://twiki.cern.ch/twiki/bin/view/LHCPhysics/CERNYellowReport-PageAt1314TeV.
[24] G. Passarino, M.J.G. Veltman, Nucl. Phys. B 160 (1979) 151.
[25] S. Kanemura, M. Kikuchi, K. Yagyu, Nucl. Phys. B 896 (2015) 80, arXiv:1502.07716 [hep-ph].
[26] T. Abe, R. Sato, K. Yagyu, J. High Energy Phys. 1507 (2015) 064, arXiv:1504.07059 [hep-ph].
[27] G. Aad, et al., ATLAS Collaboration, Phys. Rev. D 91 (2015) 012006.
[28] V. Khachatryan, et al., CMS Collaboration, Eur. Phys. J. C 75 (5) (2015) 212.